A temperature-mediated precipitation of struvite-family crystals in wastewater

S. Sutiyono[1], L. Edahwati[1], S. Muryanto[2], J. Jamari[3], A. P. Bayuseno[3]*

[1]Department of Chemical Engineering, Universitas Pembangunan Nasional "Veteran" Jawa Timur, Surabaya 60294, Indonesia
[2]Department of Chemical Engineering, UNTAG University, Bendhan Dhuwur Campus, Semarang 50233, Indonesia
[3]Department of Mechanical Engineering, Diponegoro University, Tembalang Kampus, Semarang 50275, Indonesia

Abstract : The paper presents results of the investigation into the temperature mediated mineralogical formation of struvite family crystals in a synthetic wastewater. The scale-forming solution was set-up by mixing solutions of $MgCl_2$ and $NH_4H_2PO_4$ with Mg^{+2}, NH_4^+ and PO_4^{-3} in a molar ratio (MAP) of 1:1:1. The temperature was altered: 30, 35 and 40 ^{O}C. The initial pH of the solution was set up in 9.0. SEM (equipped with EDX) analysis revealed that the crystals have a needle like-shaped morphology, and contained Mg, K, P, and O as the main composition. The Rietveld analysis of the XRPD pattern confirmed that the major phase of struvite, and struvite-(K) formed in the precipitating solids. Apparently, bobierrite and newberyte were other phosphate minerals formed at the temperature of 35 ^{O}C. Analysis of this experimental data suggested that the temperature-mediated crystallization process yielded a potential optimization of struvite precipitation.

Keywords- Bobierrite, Newberyte, Struvite, Temperature, XRPD Rietveld method.

Introduction:

Struvite ($NH_4MgPO_4·6H_2O$) is one of mineral deposits, which commonly accumulated on the surface equipment of digestion and post-digestion processes in wastewater treatment industry. The deposits present on the surface of pipes lead to create clogging problems with the inside diameter, hence generating major downtime, loss of hydraulic capacity, and increased pumping and maintenance costs[1] Nevertheless, struvite crystal potentially recovers a high amount of phosphorus and nitrogen from wastewater and subsequently it can be applied as a phosphate fertilizer[2-4]. Nowadays, struvite crystallization is a suggested method to bring down the environmentally harmful free magnesium, ammonium and phosphorus (MAP) ions in wastewater[5-9]. This method draws considerable attention because of the common occurrence of struvite in a wide variety of environments[10-16].

In the wastewater environment, struvite crystallization may be adjusted by parameters such as pH[17,18], temperature[18], rate of stirring[19,20], supersaturation[21,22], nature of phosphate materials[23-25] and the presence of foreign ions including calcium and copper[5,19,26] and sulfate[27]. Additionally, the manipulation of pH influences morphology, particle size, and thermal property of struvite[18]. Moreover, the effect of pH on thermal properties of struvite can be related to the release of volatile components during the heating process, and eventually control the relative stability of struvite. Here, an experiment on the stability of struvite can be performed at

above ambient temperature, which can provide an initial evaluation of the susceptibility to struvite decomposition for the discharge of nutrients as applied for a fertilizer[28,29].

Instead of struvite crystallization, magnesium phosphates such as $MgHPO_4 \cdot 3H_2O$ (newberyite), $Mg_3(PO_4)_2 \cdot 8H_2O$ (bobierrite) and $Mg_3(PO4)_2 22H_2O$ (cattiite) may form[13] and be related to the reduction in the concentration of free ions (Mg^{2+}, NH^{4+} and PO_4^{3-}) within the aqueous solutions[21]. For instance, the formation of struvite (S) and newberyite (N) is mainly controlled by the ion concentration and the respective supersaturation ratios of S and N[18]. As the supersaturation ratio of N/S < 2, struvite always precipitate first, while the ratio of N/S > 2 crystallization of newberyite precedes. Here the decomposition of struvite from saturated solutions is found to be dependent upon the rate of heating[30]. At a temperature below 40 °C, struvite decomposition occurs as a result of slow heating, and is accompanied by developing both ammonia and water. Nevertheless, around 80°C, struvite decomposition occurs due to the more rapid heating.

Further at the temperature of 103 °C, struvite transformation to dittmarite ($MgNH_4PO_4H_2O$) may occur in the air[31]. The subsequent transformation of struvite in water can undergo at lower temperatures of 60 °C[32]. In particular, the released remaining water and NH_4 for crystallization can occur at 235 °C and be followed by the formation of the pyrophosphate at 575 °C[31]. Here, magnesium pyrophosphate becomes the most stable phase found in the high temperature. However, the development of different minerals may be found in-between temperature. The temperature range of struvite decomposition is commonly related to the mineralogical reaction against the presence of nitrogen, air, or water[29].

The present work was undertaken to evaluate the mineralogical response to struvite formation at elevated temperatures and to quantify phosphate minerals for recovery of MAP ions. The fixed pH was selected, while the overall pH of the system was allowed to fluctuate in the removal of MAP as the thermodynamically equilibrium was achieved. This condition was set up similar to that commonly employed for struvite recovery from wastewater, where the control of pH is difficult due to economics and/or technical reasons[33-36]. The morphology and mineralogy of the solids precipitated from these solutions were determined by scanning electron microscopy (SEM) and x-ray powder diffraction (XRPD) method respectively.

Experimental:

Solution preparation for crystallization experiment:

Struvite family crystals were grown in a glass beaker mechanically stirred at 200 rpm and three sets of experimental running were performed in this study. The crystals were precipitated from stock solutions containing 0.8735 M $MgCl_2$, 0.8735 M NH_4OH, and 0.8735 M H_3PO_4 with analytical grade (Merck, Germany). The solution was subsequently diluted in 500 ml flasks so that the molar ratios of magnesium, nitrogen and phosphorus (MAP) reached up 1:1:1. The initial concentrations and molar ratios of five major ions are listed in Table I. The diluted mixing solutions were adjusted to pH 9 using 1 N KOH (analytical reagent grade). The pH solution was then measured continuously using a Beckman 44 pH meter, equipped with an Oakton pH probe at elevated temperature (30, 35 and 40 °C) and ended up for 70 min. At the end of each test, the precipitate was filtered immediately through a 0.45 μm paper filter and preserved for subsequent analysis.

Table (1): Initial concentrations and molar ratios of five major ions in the synthetic wastewater

Molar ratio & pH	Mg (mol/l)	NH₄ (mol/l)	PO₄ (mol/l)	K (mol/l)	Cl (mol/l)	Temperature
1:1:1 & 9	0.8735	0.8735	0.8735	0.8735	1.74716	30, 35, 40 °C

A saturation index (SI) was calculated to predict the mineral speciation of solid precipitated from the solution[37]. When SI > 0, the solution is supersaturated and precipitation occurs spontaneously. When SI = 0, the solution can undergo equilibrium. When SI < 0, the solution is undersaturated and no precipitation occurs. The calculation of SI for solid and dissolved phases of minerals was conducted by the visual Minteq[38].

Materials characterization of precipitates:

The scale samples were then examined by SEM on a JEOL (30 SFEG) instrument with EDX system and XRPD method. The XRPD data collection was performed using Cu-Kα monochromated radiation in a conventional Bragg-Brentano (BB) parafocusing geometry (D5005 SHIMATZU). The scan parameters (5–85 ^{O} 2θ, 0.020 steps, 15 s/step) were selected. Data were recorded digitally, and peak positions and intensities were identified either using the peak finder feature or on screen in the MATCH software. The possible crystalline phase obtained from the extensive search match was subsequently validated by the Rietveld full profile fitting analysis[39-41]. The Rietveld refinement of XRPD data was carried out by Fullprof software[42].

The XRPD Rietveld refined parameters such as: (i) the 2θ^O scale zero position, (ii) the polynomial fitting for the background with six coefficients, (iii) the phase scale factors, (iv) the cell parameters, (v) the peak asymmetry and the peak shape functions, (vi) the atomic coordinates and anisotropic temperature factors. The Fullprof program fits the diffraction line widths (FWHM) as a function of tan(θ) using the u-v-w formula of[43], while starting values of u, v and w were obtained from the values of the measured quartz. Preferred orientation of struvite was also refined, while other phases were assumed to be absent in the powder in all cases. The obtained values of the cell parameters and the calculated wt. % levels of mineralogical phases and the crystal structure models from which the full diffraction profiles are calculated by the program [39]. The calculation method is discussed in detail elsewhere[44,45].

Results and discussion:

Kinetic modelling of struvite precipitation:

Dissolution and crystallization rates of struvite were calculated using the pH measured for Mg^{2+} reduction. The crystallization rate may then be determined through either reduction of (Mg^{2+}) or increase from hydrogen ion, according to the following equation[26,35]:

$$Ln\ (C-C_{eq})= -kt +Ln\ (C-C_O) \hspace{3cm} (1)$$

Where C is the concentration of the reactant concentration at a moment t, C$_{eq}$ the reactant concentration at equilibrium, C$_O$ the initial reactant concentration, and k the kinetic constant.

Further, the evolution of pH values versus time at different temperature selected is plotted in Fig. 1. Obviously, the pH reduced slightly from an initial pH of 9.01 to approximately 8.98 < pH < 8.99 at the temperature of 30 ^{O}C and 40 ^{O}C. In contrast, at a temperature of 35 ^{O}C, the pH solution changed dramatically in the time range of 0 - 15 minutes, and subsequently remained constant. It is suggested that the solution mediated precipitation of struvite, which was completed in about 70 min.
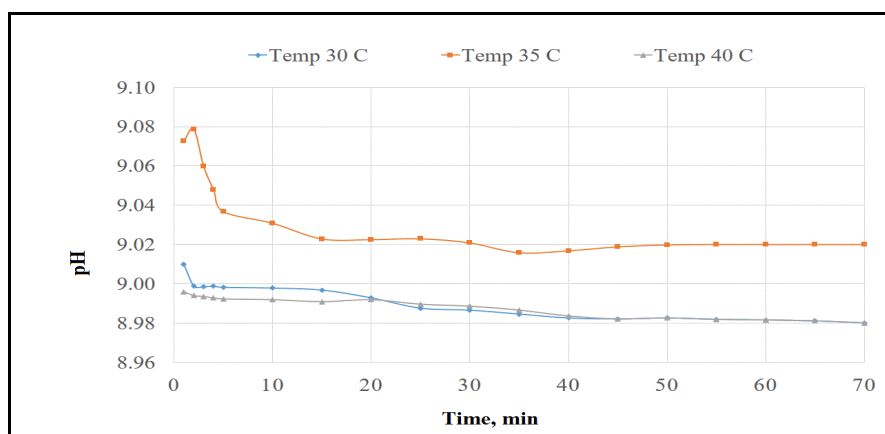

Fig. (1): Changes of pH during the mineral precipitation at the different temperatures

Moreover, the kinetics of struvite formation can be estimated from the plots of Ln [(C-Ceq)] versus time according to equation-1 (Figure 2). At the temperature solution of 30 ^{O}C, the plots revealed that the

calculated Mg concentrations fitted well with the first kinetic order model with a slope of -k, where correlation coefficients (R^2) was 0.9684. The struvite formation reaction pursued a first-order kinetic model with respect to Mg and H ions, and was in agreement with the previous findings[26,35]. Rate constants were obtained from each plot and subsequently given in Table 2. The kinetic rate constants provided a trend in that the lower temperature of the solution enabled to the lower rate constant and thus the slower precipitation occurred. Here, the kinetic constants increased from 2.952 to 12.342 h^{-1}, when the temperature increased from 30 - 40 ^{O}C. These findings suggested that the solution facilitated increasing precipitation of struvite. Further evidence for such mechanisms would be provided by quantitative XRPD analysis (Table 4).
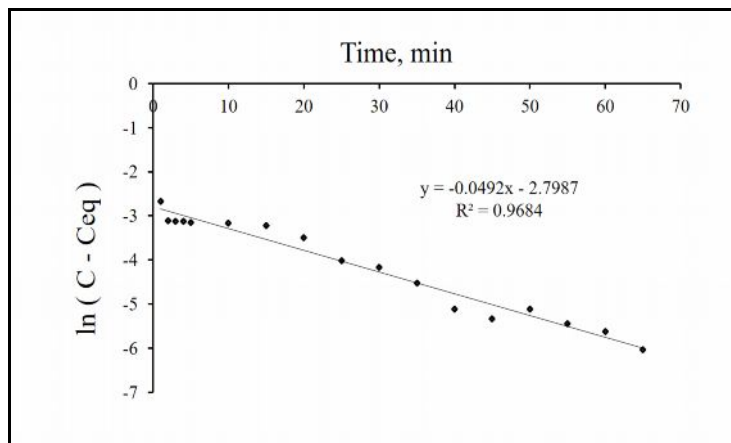

Fig. (2): The best fitted straight line through the Ln (C-C$_{eq}$) versus time for the precipitate obtained at 30 ^{O}C

Table (2): The first order rate constants for struvite crystal growth.

| Ratio of 1:1:1, pH= 9	Regression equation	Rate constant, (h^{-1})	R^2
30	Y= -0.0492x-2.7987	2.952	0.9684
35	y= -0.2057x -1.9379	12.342	0.9614
40	y= -0.2057x-1.9379	12.342	0.9614

Minerals speciation and quantitative analysis of crystal products

The mineralogy and morphology of the solids recovered from these solutions were determined by the XRPD and SEM method. This precipitate was obtained over a range of temperatures. Table 3 presented the minerals precipitated from the solution corresponding to the saturation index (SI) calculated by the visual Minteq. During the present study, the dissolution of phosphate minerals was shown to be the predominant process, approaching its maximum at the end of the period. Newberyite, struvite and struvite-(K) have the positive SI implying that those minerals could be precipitated from the solution. These findings suggested the solution mediated transformation process of struvite into different phosphate minerals (newberyite and struvite-(K)). Additionally, $Mg_3(PO_4)_2$ was also predicted to have the positive SI as precipitated minerals, while several minerals such as $Mg_2(OH)_3Cl \cdot 4H_2O$ $Mg(OH)_2$ and periclase (MgO) were undersaturated and could be not identified in the XRPD analysis. However, $Mg_3(PO_4)_2$ may be an amorphous phase and could be not detected by the XRPD search-match analysis[46].

According to the XRPD analysis, struvite and struvite-(K) can be precipitated in nearly the whole temperatures (30, 35 and 40 ^{O}C) investigated (Figure 3). The investigations performed under similar conditions also provided the appearance of sylvite. In addition, struvite always precipitated when the magnesium and phosphate concentrations were within the range of concentrations found in wastewater (Table 1) [18].

Table (3): Mineral species predicted from the visual Minteq model.

Mineral species	Solution at pH = 9; MAP molar ratio of 1:1:1		
	30	35	40
	Saturation Index (SI)		
KCl(s)	0.002	0	-0.003
$Mg(OH)_2$	-2.154	-2.183	-2.207
$Mg_2(OH)_3Cl \cdot 4H_2O$	-0.675	-0.725	-0.769
Periclase (MgO)	-4.507	-4.113	-3.728
$Mg_3(PO4)_2$	11.094	11.066	11.042
Newberyite	3.762	3.763	3.763
Struvite	8.44	8.352	8.258
Struvite (K)	5.063	5.055	5.048
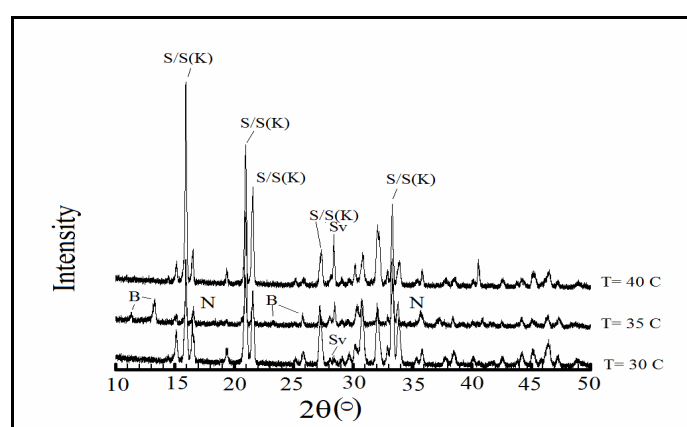
Fig. (3): XRPD trace of minerals precipitated at different temperature. The peaks are labelled B (bobierrite), N (newberyite), S (struvite), S(K) (struvite-K) and Sv (sylvite).

Further struvite growth and its thermodynamic stability generally depend on the neutral or basic aqueous solutions[21,22]. Our work has demonstrated that, within a narrow range temperature and the initial equimolar concentrations of MAP similar to those found in wastewater, struvite family crystals could be precipitated simultaneously[46]. The stability for such mixture of minerals depends on the pH of the system. At pH <6.0, newberyite has the stable form. In this condition, struvite may readily transform into newberyite, while both struvite and bobierrite are stable phases for alkaline pH[47]. However, struvite decomposition depends not only on supersaturation regarded to the minerals, but also on the ammonia activity in the solution. Thus struvite, bobierrite and newberyite may coexist under certain conditions in wastewater[46].

In the present study, only bobierrite and newberyite were obtained with struvite in the precipitates at the temperature of 35 °C. The apparent equilibrium of both phosphate minerals with struvite may occur at this temperature and pH 9. The observations from this work also provided that struvite may partially transform to bobierrite and newberyite due to the ammonia activity in the solution[46] and the simultaneous formation of the two solid phases may occur in a limited concentration range and pH[33].

The characteristic morphologies obtained in the experiments at the temperature of 30 °C are given in Figure 4. Struvite occur as needle like crystal as shown in the SEM micrograph[33]. The EDX analysis presented the respective peak intensities of P, Mg, K, Cl and O, which were composed to struvite and struvite-(K) in addition to sylvite.
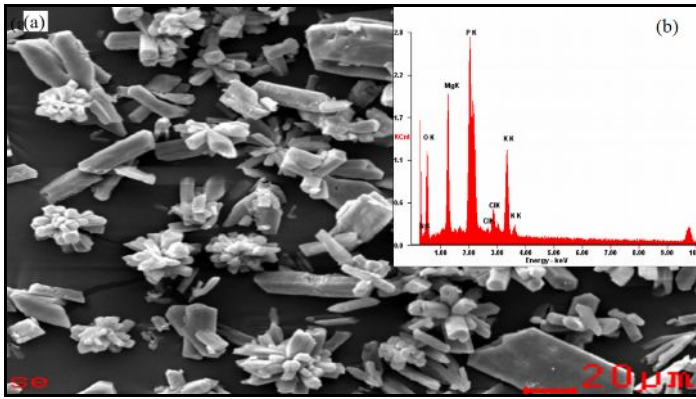
Fig. (4): (a) SEM micrograph, (b) EDX analysis of struvite family crystals precipitated at pH 9 as the molar ratio of 1: 1: 1 at 30 ^{O}C.

Detailed XRPD quantitative analyses were also performed on the scale samples. Table 4 gives the mineralogical phase composition of the precipitates at the different temperature. At the temperature of 30 ^{O}C, 37.9 wt. % of struvite and 61.6 wt. % of struvite-(K) were detected along with sylvite (0.5 wt.%) as impurity in solids precipitated. Chloride components in solution may associate with the stock solution, resulting in impurities in the recovered precipitate[48]. A quite abundance of struvite was also found to increase in the elevated temperature. The corresponding to the process observed at 35 ^{O}C, the high content of bobierrite, struvite-(K) and newberyite was found as the crystallized product. Accordingly, the struvite crystal products became less and the small amount of impurities such as $MgCl_2$ and sylvite was still produced. The investigations performed under similar conditions at the temperature of 40 ^{O}C showed only the appearance of struvite and struvite-(K) in addition to sylvite. Predominantly, the high amount of struvite and struvite-(K) can be precipitated within the temperature observed.

Table (4): XRPD results on the mineral deposits formed from the synthetic wastewater.

| Mineral | MAP molar ratio of 1:1:1 | | | Crystal structure model |
| | Temperature solution (^{O}C) | | | |
	30	35	40	
Struvite	37.9 (6)*	45.5(4)	54.5 (6)	Whitaker and Jeffery (1970) [52]
Struvite (K)	61.6 (8)	18.6(6)	42.4 (6)	Graeser et al. (2008)[53]
Sylvite	0.5 (4)	1.2(5)	3.1 (6)	Ott (1926)[54]
Newberyite		5.1(3)		Abbona and Boistelle (1979) [51]
$MgCl_2$		0.2(1)		Busing (1970) [55]
Bobierrite [$Mg_3(PO4)_2 \cdot 8H_2O$]		29.4(5)		Takagi et al. (1986) [47]

*Figures in parentheses indicate the least-squares estimated standard deviation (esd) referring to the least significant figure to left

The purity of struvite with respect to additional mineralogical components and the association of contaminants may be controlled by temperature. In batch experiments conducted over the temperature range of 30-40 ^{O}C, the temperature was found to be the primary factor affecting the production of struvite[49,50]. Additionally, the temperature (30, 35 and 40 ^{O}C) selected in the present study may be a typical range of optimal temperature on the physical and chemical properties of struvite precipitated from $MgCl_2$-$(NH_4)_2HPO_4$-KOH-H_2O system[49]. This system could also provide fundamental information about the effect of temperature on struvite formation in the more complex solutions[33-36]. Moreover, findings from the XRPD Rietveld method and simultaneous prediction of minerals speciation using the visual Minteq provided validation into the influence of temperature on the amount of struvite crystal produced. In turn, the present results can be adopted as a strategy to ultimately improve the phosphate recovery from wastewater.

Conclusion:

It can be concluded that temperature controlled precipitation of struvite from the wastewater and was the limiting factor on the precipitation reaction kinetics. The rate of disappearance of Mg^{2+} in the solutions increased with increasing temperature. The estimated rate constants were from 2.952 to 12.342 h^{-1}, in the temperature range of 30-40 ^{O}C, as the constant MAP molar ratio of 1:1:1. The experimental observations with different temperature indicated a great mixture of phosphate minerals obtained in this solution. Struvite and struvite-(K) where the major minerals crystallized in the solution at 30°C. In addition to both minerals, bobierrite and newberyite can be precipitated, as the temperature was increased from 30 to 35 ^{O}C. The solution with the temperature of 40 ^{O}C has the effect on the struvite and struvite-(K) precipitation, while the small impurity of sylvite was always found in any precipitates found during the experiments.

Acknowledgment

References

1. Doyle JD, Simon AP. Struvite formation, control and recovery. Water Res., 2002, 36; 3925-3940.
2. Ponce RG, De Sa MEGL. Evaluation of struvite as a fertilizer: a comparison with traditional P sources. Agrochimica. 2007, 51; 301-308.
3. Sudha R, Premkumar P. Lead Removal by Waste Organic Plant Source Materials Review. International Journal of ChemTech Research, 2016, 9 (01); 47-57.
4. Kouame Kouame Victor, Meite Ladji, Adjiri Oi Adjiri, Yapi Dope Armel Cyrille, Tidou Abiba Sanogo, Bioaccumulation of Heavy Metals from Wastewaters (Pb, Zn, Cd, Cu and Cr) in Water Hyacinth (*Eichhornia crassipes*) and Water Lettuce (*Pistia stratiotes*). International Journal of ChemTech Research, 2016, 9 (02); 189-195.
5.   Hao XD, Wang CC, Lan L, Van Loosdrecht MCM. Struvite formation, analytical methods and effects of pH and Ca^{2+}. Water Sci. Technol., 2008, 58;1687-1692.
6. Kim D, Ryu HD, Kim MS, Kim J, Lee SI. Enhancing struvite precipitation potential for ammonia nitrogen removal in municipal landfill leachate. J. Hazard. Mater., 2007, 146; 81-85.
7.   Senthamil Selvan K, Palanivel M. A Case study approach on Municipal Solid Waste generation and its impact on the soil environment in Dharapuram Municipality, Tamilnadu, India. International Journal of ChemTech Research, 2016, 9 (02); 196-204.
8. Lina Rose Varghese and Nilanjana Das. Application of nano-biocomposites for remediation of heavy metals from aqueous environment: An Overview. International Journal of ChemTech Research, 2015, 8 (2); 566-571.
9. Diwani GE, Rafie SE, Ibiari NNE, Aila, HIE. Recovery of ammonia nitrogen from industrial wastewater treatment as struvite slow releasing fertilizer. Desalination. 2007, 214; 200-214.
10. Archana S, Jaya Shanthi R. Removal of Cr (VI) from tannery effluent using synthesized polyphenylenediamine nanocomposites. International Journal of ChemTech Research, 2015, 8 (5); 85-89.
11. Kouame Kouame Victor, Meite Ladji, Adjiri Oi Adjiri, Yapi Dope Armel Cyrille, Tidou Abiba Sanogo. Bioaccumulation of Heavy Metals from Wastewaters (Pb, Zn, Cd, Cu and Cr) in Water Hyacinth (*Eichhornia crassipes*) and Water Lettuce (*Pistia stratiotes*). International Journal of ChemTech Research, 2016, 9 (02); 189-195.
12. Naga Babu A, Krishna Mohan GV, Ravindhranath K. Removal of Chromium (VI) from Polluted waters using Adsorbents derived from Chenopodium album and Eclipta prostrate Plant Materials. International Journal of ChemTech Research, 2016, 9(03); 506-516.
13. Michałowski T, Pietrzyk A. A thermodynamic study of struvite+water system. Talanta. 2007, 68; 594-601.
14. Xiu-Fen L, Barnes D, Jian C. Performance of struvite precipitation during pretreatment of raw landfill leachate and its biological validation. Environ. Chem. Lett., 2011, 9; 71-75.

15. Ahmed Hassan Alamin, Lupong Kaewsichan. Adsorption of Zn(II) and Cd(II) ions from aqueous solutions by Bamboo biochar cooperation with Hydroxyapatite and Calcium Sulphate. International Journal of ChemTech Research, 2015, 7(5); 2159-2170.

16. Sangeetha K, Vasugi G, Girija EK. Removal of lead ions from aqueous solution by novel hydroxyapatite/alginate/gelatin composites. International Journal of ChemTech Research, 2015, 8 (5); 117-125.

17. Zhang T, Ding L, Ren H, Xiong X. Ammonium nitrogen removal from coking wastewater by chemical precipitation recycle technology. Water Res., 2009, 43; 5209-5215.

18. Abbona F, Madsen HEL, Boistelle R. Crystallization of two magnesium phosphates, struvite and newberyite: effect of pH and concentration, J. Cryst. Growth., 1982, 57; 6-14.

19. Kim D, Kim J, Ryu HD, Lee SI. Effect of mixing on spontaneous struvite precipitation from semiconductor wastewater. Bioresour. Technol., 2009, 100; 74-78.

20. Wilsenach JA, Schuurbiers CAH, van Loosdrecht MCM. Phosphate and potassium recovery from source separated urine through struvite precipitation. Water Res., 2007, 41; 458-466.

21. Ali MI, Schneider PA. An approach of estimating struvite growth kinetic incorporating thermodynamic and solution chemistry, kinetic and process description, Chem. Eng. Sci., 2008, 63; 3514-3525.

22. Ren L, Schuchardt F, Shen Y, Li G, Li C. Impact of struvite crystallization on nitrogen losses during composting of pig manure and cornstalk. Waste Manage., 2010, 30; 885-892.

23. Mohammad Athiq M, Abhishek B, Saranya D, Rohit KC, Prashanth Kumar HP. Application of Bio technology in Treatment of Heavy Metal Contaminated Industrial Waste Water-A case study. International Journal of ChemTech Research, 2015, 8 (5); 144-147.

24. Malathi S, Srinivasan K, Gomathi M. Studies on the removal of Cr (VI) from aqueous solution by activated carbon developed from Cottonseed activated with sulphuric acid. International Journal of ChemTech Research, 2015, 8 (2); 795-802.

25. Parsons SA, Smith JA. Phosphorus removal and recovery from municipal wastewaters. Elements. 2008, 4; 109-112.

26. Muryanto S, Bayuseno AP. Influence of Cu^{2+} and Zn^{2+} as additives on crystallization kinetics and morphology of struvite. Powder Technol., 2014, 253; 602-607.

27. Kabdasli I, Parsons SA, Tunay O. Effect of major ions on induction time of struvite precipitation. Croat. Chem. Acta., 2006, 79; 243-251.

28. Andrade A, Schuiling RD. The chemistry of struvite crystallization. Mineral. J., (Ukraine). 2001, 23; 37-46.

29. Frost R, Weier M, Erickson KL. Thermal decomposition of struvite. J. Therm. Anal. Calorim., 2004, 76; 1023-1033.

30. Hanhoun M, Montastruc L, Azzaro-Pantel C, Biscans B, Freche M, Pibouleau L. Temperature impact assessment on struvite solubility product: a thermodynamic modeling approach. Biochem. Eng. J., 2011, 167; 50-58.

31. Abdelrazig BEI, Sharp JH. Phase changes on heating ammonia magnesium phosphate hydrates, Thermochimica Acta., 1988, 129; 197-215.

32. Sarkar AK. Hydration/dehydration characteristics of struvite and dittmarite pertaining to magnesium ammonium phosphate cement systems. J. Mater. Sci., 1991, 26; 2514-2518.

33. Babić-Ivančić V, Kontrec J, Brečević L, Kralj D. Kinetics of struvite to newberyite transformation in the precipitation system $MgCl_2$-$NH_4H_2PO_4$-$NaOH$-H_2O. Water Res., 2006, 40; 3447-3455.

34. Etter B, Tilley E, Khadka R, Udert KM. Low-cost struvite production using source-separated urine in Nepal. Water Res., 2011, 45; 852-862.

35. Nelson NO, Mikkelsen RL, Hesterberg DL. Struvite precipitation in anaerobic swine lagoon liquid: effect of pH and Mg:P ratio and determination of rate constant. Bioresour. Technol., 2003, 89; 229-236.

36. Ronteltap M, Maurer M, Gujer W. Struvite precipitation thermodynamics in source-separated urine. Water Res., 2007, 41; 977-984.

37. Ye Z, Shen Y, Ye X, Zhang Z, Chen S, Shi J. Phosphorus recovery from wastewater by struvite crystallization: Property of aggregates. J. Environ. Sci., 2014, 26; 991-1000.

38. USEPA (1991). A geochemical assessment model for environmental systems: Version 3.0 user manual. U.S.EPA.EPA/600/3-91/021. Washington, DC.

39. Hill RJ, Howard CJ. Quantitative phase analysis from neutron powder diffraction data using the Rietveld method. J. Appl. Crystallogr., 1987, 20; 467-474.

40. Rietveld HM. A profile refinement method for nuclear and magnetic structures. J. Appl. Crystallogr., 1969, 2; 65-71.

41. Winburn RS, Grier DG, McCarthy GJ, Peterson RB. Rietveld quantitative X-ray diffraction analysis of NIST fly ash standard reference materials. Powder Diffr., 2000, 15; 163-172.

42. Rodriguez-Carvajal J. Program Fullprof. 2k, version 3.30, Laboratoire Leon Brillouin, France, June 2005.

43. Caglioti G, Paoletti A, Ricci FP. Choice of collimator for a crystal spectrometer for neutron diffraction. Nucl. Instrum. Methods. 1958, 35; 223-228.

44. Bayuseno AP, Schmahl WW. Improved understanding of the pozzolanic behaviour of MSWI fly ash with $Ca(OH)_2$ solution. Int. J. Environ. Waste Manage. 2015, 15; 39-66.

45. Mahieux P.-Y., Aubert J-E., Cyr M., Coutand M, Husson B. Quantitative mineralogical composition of complex mineral wastes-contribution of the Rietveld method. Waste Manage., 2010; 30, 378-388.

46. Bhuiyan MIH, Mavinic DS, Koch FA. Thermal decomposition of struvite and its phase transition. Chemosphere. 2008, 70; 1347-1356.

47. Takagi S, Mathew M, Brown WE. Crystal structures of bobierrite and synthetic $Mg_3(PO_4)_2 \cdot 8H_2O$. Am. Mineral., 1986, 71; 1229 -1233.

48. Rouff AA. Sorption of chromium with struvite during phosphorus recovery. Environ. Sci. Technol., 2012, 46; 12493-12501.

49. Stratful I, Scrimshaw MD, Lester JN. Conditions influencing precipitation of magnesium ammonium phosphate. Water Res., 2001, 35; 4191-4199.

50. Ma N, Rouff AA. Influence of pH and oxidation state on the interaction of arsenic with struvite during mineral formation. Environ. Sci. Technol., 2012, 46; 8791-8798.

51. Abbona F, Boistelle R. Growth morphology and crystal habit of struvite crystals ($MgNH_4PO_4 \cdot 6 H_2O$). J. Cryst. Growth. 1979, 46; 339-354.

52. Whitaker A, Jeffery JW. The crystal structure of struvite, $MgNH_4PO_4 \cdot 6H_2O$. Acta Crystallogr., 1970, B26;1429-1440.

53. Graeser S, Postl W, Bojar H-P, Berlepsch P, Armbruster T, Raber T, Ettinger K, Walter F. Struvite-(K), $KMgPO_4 \cdot 6H_2O$, the potassium equivalent of struvite a new mineral. Eur. J. Mineral., 2008, 20; 629-633.

54. Ott H. Die Strukturen von Mn O, Mn S, Ag F, Ni S, Sn I4, Sr Cl_2, Ba F_2, praezisions messungen einiger alkalihalogenide. Z. Kristallogr., 1926, 63; 222-230.

55. Busing WR. An interpretation of the structures of alkaline earth chlorides in terms of interionic forces. T. Am. Crystallogr. Assoc., 1970, 6; 57-72.

*****